JACS
JOURNAL OF THE AMERICAN CHEMICAL SOCIETY

COMMUNICATION

pubs.acs.org/JACS

Highly Crystalline Nanofilm by Layering of Porphyrin Metal−Organic Framework Sheets

Soichiro Motoyama,[†,‡] Rie Makiura,[*,§,∥] Osami Sakata,[∥,⊥] and Hiroshi Kitagawa[*,†,‡,∥]

[†]Division of Chemistry, Graduate School of Science, Kyoto University, Kyoto 606-8502, Japan
[‡]Department of Chemistry, Faculty of Science, Kyushu University, Fukuoka 812-8581, Japan
[§]Nanoscience and Nanotechnology Research Center, Osaka Prefecture University, Osaka 599-8531, Japan
[∥]CREST, Japan Science and Technology Agency, Tokyo 102-0075, Japan
[⊥]Japan Synchrotron Radiation Research Institute/SPring-8, Hyogo 679-5198, Japan

Supporting Information

ABSTRACT: Layer-structured metal−organic framework (MOF) nanofilms (NAFS-2) consisting of 5,10,15,20-tetrakis(4-carboxyphenyl)porphyrin (H_2TCPP) molecules and copper ion metal linkers were assembled on a gold or a silicon surface by applying a solution-based layer-by-layer growth technique coupled with the Langmuir−Blodgett method. Synchrotron X-ray diffraction measurements showed that NAFS-2 exhibits highly crystalline order in both the in-plane and out-of-plane orientations. Each MOF sheet (monolayer) adheres without pillaring units, and the nanofilm maintains its highly crystalline order above 200 °C. The results provide an excellent demonstration of how to exercise in a facile way fine control of the assembly of molecule-based hybrid objects and their thermal stability, which is a key issue for the future use of MOFs in potential applications in nanodevices.

The rational design and construction of functional layered systems on surfaces whose structures are finely controlled at the nanoscale represent a key objective of modern materials science and a key challenge for creating future nanodevices.[1,2] Coordination materials are excellent candidates as building blocks of such nanoarchitectures because the rich variety of their components, metal ions and organic ligands, offers a vast number of combination possibilities to generate well-designed structures and functionalities. In the past decade, metal−organic frameworks (MOFs), which are highly crystalline porous coordination polymers, have attracted considerable attention because they exhibit various unique properties such as gas sorption, molecular separation, storage, and catalysis associated with their highly regularized pores in the bulk-crystal state.[3,4] To utilize MOFs or related coordination materials in nanotechnological devices such as sensors and catalysts, their fabrication in the film state has been actively pursued[5] through direct crystal growth from solvothermal solution[6] or by step-by-step liquid epitaxial growth.[7]

We very recently reported an unconventional solution-based, ambient-conditions film fabrication technique involving layer-by-layer deposition coupled with the Langmuir−Blodgett method (LB-LbL), which resulted in a preferentially oriented MOF nanofilm (NAFS-1) on a silicon substrate.[8] An important issue in exploring the potential of this technique is to demonstrate its versatility to provide diverse types of well-ordered nanofilms of controllable structure and size at the nanoscale on various substrates. Examination of the thermal stability of such highly crystalline nanofilms is also of paramount importance. Here we changed the molecular building units (in the absence of pillaring molecules) to modify the interlayer spacing of a MOF nanofilm while keeping the molecular arrangement of the layer intact and explored its structural integrity upon annealing using the synchrotron X-ray diffraction (XRD) technique. In addition, the NAFS-2 nanofilm growth was achieved on both gold and silicon substrates, opening the way for their integration as electrodes for nanodevices.

Porphyrin derivatives have been extensively employed as versatile components in the topological design of two-dimensional (2D) and three-dimensional (3D) extended porous networks and widely studied because of their varied and rich chemical and physical properties.[2,4,7g,8] We applied the LB-LbL technique using a free-base porphyrin, 5,10,15,20-tetrakis(4-carboxyphenyl)porphyrin (H_2TCPP), as shown schematically in Figure 1. Spreading a solution of H_2TCPP in toluene/ethanol onto a $CuCl_2$ aqueous solution subphase and compressing the molecules on the surface (the LB method) led to the assembly of 2D H_2TCPP arrays mediated by copper ions (H_2TCPP−Cu). The observed surface pressure−area (π−A) isotherm for H_2TCPP−Cu (Figure S1 in the Supporting Information) was identical to that in NAFS-1,[8] which consists of CoTCPP−Cu arrays and pyridine pillaring molecules; this indicates that H_2TCPP−Cu has the same molecular arrangement in the sheet as the CoTCPP−Cu LB film. However, we note that the H_2TCPP−Cu sheet can accommodate water molecules in the available coordinatively unsaturated axial sites of the copper units, while in NAFS-1, the pyridine molecules (used as the third structure-directing component) protrude from the CoTCPP−Cu plane. The H_2TCPP−Cu sheets were then subjected to an intermediate rinse and solvent immersion process, resulting in the formation of a layer-structured nanofilm designated as NAFS-2 (*na*nofilm of metal−organic *f*rameworks on *s*urfaces no. 2). Successive LbL sheet stacking of NAFS-2 was

Received: November 30, 2010
Published: March 30, 2011

dx.doi.org/10.1021/ja110720f | J. Am. Chem. Soc. 2011, 133, 5640–5643

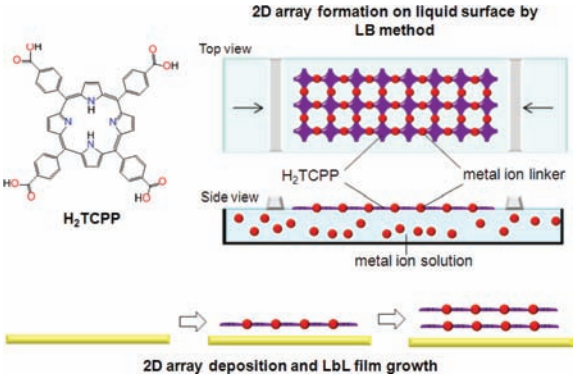

Figure 1. Schematic illustration of the representative assembly processes of NAFS-2 involved in the combined Langmuir−Blodgett/layer-by-layer (LB-LbL) nanofilm growth technique.

confirmed by monitoring the UV−vis (Figures S2 and S3) and IR (Figures S4 and S5) spectra of the nanofilms after each deposition cycle. The films were also characterized by X-ray photoelectron spectroscopy (XPS) (Figure S6).

XRD measurements on NAFS-2 nanofilms were performed using synchrotron X-ray radiation. The XRD profiles (λ = 1.555 Å) for different scattering geometries of a 50-layer NAFS-2 film (NAFS-2_50L) and the derived structural model are shown in Figure 2. XRD measurements using the out-of-plane scattering geometry, which is sensitive to the lattice parameters parallel to the film growth direction, were carried out, and Figure 2a shows the out-of-plane XRD pattern of NAFS-2 collected by $\theta-2\theta$ scans. Two diffraction peaks indexed as (001) and (002) were observed, revealing the highly ordered layer-stacking manner of the nanofilm (Figures S7−S10) and leading to a value of 7.026(3) Å for the size of the interlayer spacing, *c*, for NAFS-2 (Figure 2c). The calculated out-of-plane XRD pattern and the peak positions [including only (00*l*) reflections] are also included in Figure 2a. The *c* value in NAFS-2 is significantly smaller than the interlayer spacing observed in NAFS-1 [*c* = 9.380(3) Å],[8] and the substantial interlayer collapse in NAFS-2 can be attributed to the absence of pyridine molecules. In NAFS-1, these coordinated axially to both the copper binuclear blocks and CoTCPP and projected outward from each sheet.[8] On the other hand, water molecules are available in NAFS-2 to coordinate to the axial sites of the binuclear $Cu_2(COO)_4$ paddle-wheel units to complete the coordination sphere. The estimated $H_2TCPP-Cu$ layer thickness taking into account such axially coordinated water molecules (i.e., the distance between hydrogen atoms of the coordinated water molecules across each sheet) is ~7.6 Å, which is slightly larger than the NAFS-2 interlayer spacing obtained from the XRD measurements. This is consistent with a sheet layering pattern in which consecutive sheets do not stack directly on top of each other along *c* (i.e., an AA stacking sequence) but are arbitrarily off-registered (i.e., an AB pattern) (Figure 2c), placing neighboring axially coordinated water molecules in the interlayer space away from each other and leading to a smaller interlayer distance than the magnitude of the film thickness estimated by considering the bound water molecules. The average tilting angle of the stacked layers was estimated to be ~3° from a rocking curve scan (θ scan) at the (001) peak position (Figure S8). The larger tilting angle than in NAFS-1 (0.3°)[8] can be attributed to the weaker interaction between the

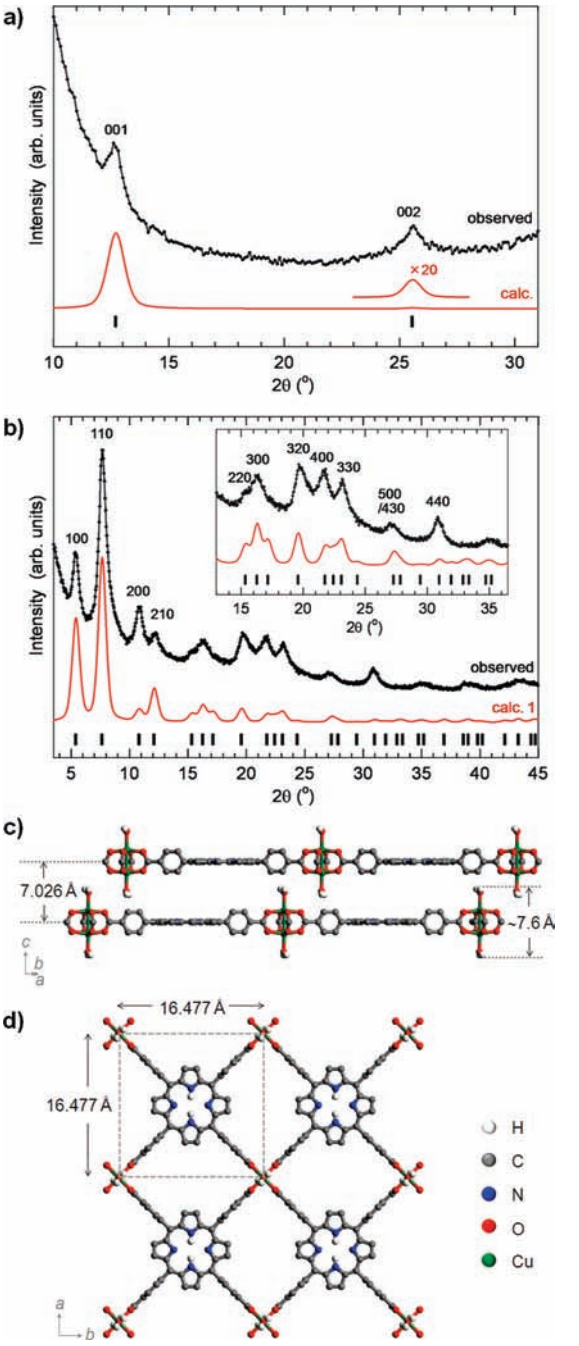

Figure 2. (a, b) Synchrotron XRD profiles (black circles, λ = 1.555 Å) of a NAFS-2 thin film on a gold substrate obtained in (a) the out-of-plane direction by using a $\theta-2\theta$ scattering geometry and (b) the in-plane direction with a detection angle of 0.21° with respect to the surface. The reflection positions (black bars) and the simulated profiles (red solid lines) obtained using the constructed structural model for NAFS-2 depicted in (c) and (d) are also included. (c, d) Schematic diagrams of the proposed crystalline structure of NAFS-2. H atoms are shown in white, C in gray, N in blue, O in red, and Cu^{2+} in green. Some H atoms have been omitted for clarity.

layers, as there are no "layer-locking" molecules protruding from the sheets to exercise stereoelectronic control in NAFS-2.

The grazing-incidence XRD (GIXRD) technique (in-plane scattering geometry), which is sensitive to the lattice parameters

dx.doi.org/10.1021/ja110720f |*J. Am. Chem. Soc.* 2011, 133, 5640–5643

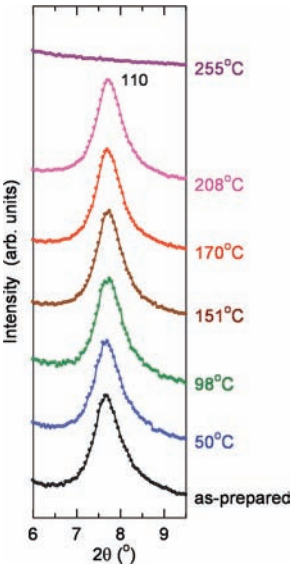

Figure 3. GIXRD profiles (λ = 1.555 Å) of the as-prepared NAFS-2 film on a gold substrate and of the same film after heating at various temperatures to 255 °C in the vicinity of the (110) Bragg reflection. Observation of diffraction peaks above 200 °C confirmed that NAFS-2 maintains its highly crystalline state at high temperatures (also see Figure S15).

parallel to the substrate plane, was employed with an incidence angle (α) of 0.21° for the same NAFS-2 nanofilms. The observation of sharp diffraction peaks in the in-plane XRD profile (Figure 2b) indicated that NAFS-2 is highly crystalline in the substrate-plane direction, and all of the reflections could be indexed as (*hk*0) [also see the profile fitting of the GIXRD data (Figure S11) and the complementary GIXRD data on NAFS-2 films with different numbers of layers (Figures S7−S10) and on a silicon(100) substrate (Figure S12)]. The derived basal plane dimensions [$a = b$ = 16.477(2) Å for NAFS-2_50L] of the pseudo-2D tetragonal unit cell of NAFS-2 are comparable to those of NAFS-1 (16.46 Å)[8] and bulk porphyrin MOFs built from MTCPP units (~16.6 Å).[4a,b] This provides unambiguous evidence that the highly ordered in-plane molecular arrangement in NAFS-2 consists of a "checkerboard" motif of H_2TCPP units linked by binuclear $Cu_2(COO)_4$ paddle wheels, the latter comprising copper ions and the carboxylic acid substituent groups of H_2TCPP (Figure 2d). The presence of the $Cu_2(COO)_4$ units in NAFS-2 was also confirmed by IR spectroscopy (Figures S4 and S5). In-plane XRD measurements of NAFS-2 formed on a Si(100) substrate were also carried out, and the consistency of the observed profile (Figure S12) shows that NAFS-2 can easily be fabricated on different substrates while retaining the same crystalline structure. Simulations of the in-plane XRD pattern [including only (*hk*0) peaks] were carried out using the NAFS-2 structural model (AB stacking pattern with B representing an arbitrary sheet orientation relative to A; calc. 1 in Figure 2b) that was discussed earlier for the out-of-plane diffraction results, and the results were found to be in good agreement with experiment. On the other hand, the calculated in-plane pattern for an AA stacking motif (calc. 2) shown in Figure S13 led to inferior agreement with the experimental results: the clear observation in the experimental profile of the (200) and (300) Bragg reflections, which appear in calc. 1 but are absent in calc. 2, supports the idea that the sheets in NAFS-2 are layered in an off-aligned manner along the interlayer direction, as we also concluded on the basis of the out-of-plane XRD results. The average crystalline domain size was evaluated as ~20 nm from the peak width of the intense (110) reflection. Atomic force microscopy (AFM) images of the NAFS-2 film also showed domains whose size is ~20 nm (Figure S14).

The thermal stability of NAFS-2 was studied by ex-situ synchrotron GIXRD. The NAFS-2 film was first annealed on a hot plate at selected temperatures, and then in-plane XRD patterns (Figure 3) were collected after the film was allowed to cool to room temperature. Observation of Bragg reflections provided unambiguous evidence that NAFS-2 retains its highly crystalline order up to temperatures above 200 °C; decomposition occurred at 240 °C, where the intense (110) reflection disappeared (also see Figure S15). Survival of the $Cu_2(COO)_4$ paddle-wheel coordination linkage in NAFS-2 to these high temperatures was also supported by IR spectroscopy measurements (Figure S16).

In summary, we have reported the facile fabrication of highly crystalline MOF nanofilms (NAFS-2) under mild conditions on both gold and silicon surfaces. The interlayer spacing in NAFS-2 was varied while retaining the same in-plane molecular arrangement by employing different molecular building units than for the previously reported NAFS-1. This provided an excellent demonstration of the power and versatility of the LB-LbL film growth strategy, which here allowed the construction of nanofilms that were well-ordered in both the out-of-plane and in-plane orientations using only two simple components (free-base porphyrin molecular building blocks and metal-ion joints) and no pillaring units. The (110) Bragg reflection in the XRD profile of NAFS-2 survived even after annealing at high temperatures, implying that the nanofilm maintains its high crystallinity above 200 °C. Finally, because the constituent layers of the nanofilm adhere only weakly to each other, removal of the axially coordinated water molecules and introduction of suitable additional components into NAFS-2 should allow further fine-tuning of the stacking motif and the interlayer spacing as well as their efficient selective absorption, inducing catalytic reactions[9] at the available axial sites.

■ ASSOCIATED CONTENT

Supporting Information. Sample preparation; UV−vis, IR, and XPS spectra; XRD patterns; and AFM images of the samples. This material is available free of charge via the Internet at http://pubs.acs.org.

■ AUTHOR INFORMATION

Corresponding Author

r-makiura@21c.osakafu-u.ac.jp; kitagawa@kuchem.kyoto-u.ac.jp

■ ACKNOWLEDGMENT

We thank JSPS (Grants-in-Aid for Scientific Research 20350030, 20655030, 22108524, and 22750056), MEXT "Special Coordination Funds for Promoting Science and Technology (SCF)", and the Global COE Program "Science for Future Molecular Systems" for financial support; SPring-8 for access to the synchrotron X-ray facilities under the Priority Nanotechnology Support Program administered by JASRI (2009B1772, 2010A1188); and the Center of Advanced Instrumental Analysis,

Kyushu University, for the use of the FT-IR spectrometer and the ESCA system.

REFERENCES

(1) (a) Moore, R. G.; Zhang, J.; Nascimento, V. B.; Jin, R.; Guo, J.; Wang, G. T.; Fang, Z.; Mandrus, D.; Plummer, E. W. *Science* **2007**, *318*, 615. (b) Huang, X.; Li, J. *J. Am. Chem. Soc.* **2007**, *129*, 3157. (c) Franceschi, S. D.; Kouwenhoven, L.; Schönenberger, C.; Wernsdorfer, W. *Nat. Nanotechnol.* **2010**, *5*, 703. (d) Zhu, Y.; Tour, J. M. *Nano Lett.* **2010**, *10*, 4356.

(2) (a) Qian, D. J.; Nakamura, C.; Miyake, J. *Langmuir* **2000**, *16*, 9615. (b) Qian, D. J.; Nakamura, C.; Miyake, J. *Chem. Commun.* **2001**, 2312. (c) Bélanger, S.; Hupp, J. T. *Angew. Chem., Int. Ed.* **1999**, *38*, 2222. (d) Lee, C. Y.; She, C.; Jeong, N. C.; Hupp, J. T. *Chem. Commun* **2010**, *46*, 6090.

(3) (a) Yaghi, O. M.; O'Keeffe, M.; Ockwig, N. W.; Chae, H. K.; Eddaoudi, M.; Kim, J. *Nature* **2003**, *423*, 705. (b) Férey, G. *Chem. Soc. Rev.* **2008**, *37*, 191. (c) Kitagawa, S.; Kitaura, R.; Noro, S. *Angew. Chem., Int. Ed.* **2004**, *43*, 2334. (d) Li, Q.; Zhang, W.; Miljanic, O. S.; Sue, C. H.; Zhao, Y. L.; Liu, L.; Knobler, C. B.; Stoddart, J. F.; Yaghi, O. M. *Science* **2009**, *325*, 855. (e) Okawa, H.; Shigematsu, A.; Sadakiyo, M.; Miyagawa, T.; Yoneda, K.; Ohba, M.; Kitagawa, H. *J. Am. Chem. Soc.* **2009**, *131*, 13516. (f) Long, J. R.; Yaghi, O. M. *Chem. Soc. Rev.* **2009**, *38*, 1213 and references cited therein. (g) Hindson, K. *Eur. J. Inorg. Chem.* **2010**, 3683 and references cited therein.

(4) (a) Choi, E. Y.; Barron, P. M.; Novotny, R. W.; Son, H. T.; Hu, C.; Choe, W. *Inorg. Chem.* **2009**, *48*, 426. (b) Chung, H.; Barron, P. M.; Novotny, R. W.; Son, H.-T.; Hu, C.; Choe, W. *Cryst. Growth Des.* **2009**, *9*, 3327. (c) Barron, P. M.; Wray, C. A.; Hu, C.; Guo, Z.; Choe, W. *Inorg. Chem.* **2010**, *49*, 10217. (d) Shultz, A. M.; Farha, O. K.; Hupp, J. T.; Nguyen, S. T. *J. Am. Chem. Soc.* **2009**, *131*, 4204. (e) Goldberg, I. *Chem.—Eur. J.* **2000**, *6*, 3863. (f) Posner, Y. D.; Patra, G. K.; Goldberg, I. *Eur. J. Inorg. Chem.* **2001**, 2515. (g) Shmilovits, M.; Posner, Y. D.; Vinodu, M.; Goldberg, I. *Cryst. Growth Des.* **2003**, *3*, 855. (h) Shmilovits, M.; Vinodu, M.; Goldberg, I. *Cryst. Growth Des.* **2004**, *4*, 633. (i) Lipstman, S.; Goldberg, I. *J. Mol. Struct.* **2008**, *890*, 101. (j) Carlucci, L.; Ciani, G.; Proserpioa, D. M.; Portab, F. *CrystEngComm* **2005**, *7*, 78. (k) Sato, T.; Mori, W.; Kato, C. N.; Yanaoka, E.; Kuribayashi, T.; Ohtera, R.; Shiraishi, Y. *J. Catal.* **2005**, *232*, 186. (l) Kato, C. N.; Ono, M.; Hino, T.; Ohmura, T.; Mori, W. *Catal. Commun.* **2006**, *7*, 673.

(5) Zacher, D.; Shekhah, O.; Wöll, C.; Fischer, R. A. *Chem. Soc. Rev.* **2009**, *38*, 1418.

(6) (a) Hermes, S.; Schroder, F.; Chelmowski, R.; Wöll, C.; Fischer, R. A. *J. Am. Chem. Soc.* **2005**, *127*, 13744. (b) Biemmi, E.; Scherb, C.; Bein, T. *J. Am. Chem. Soc.* **2007**, *129*, 8054. (c) Gascon, J.; Aguado, S.; Kapteijn, F. *Microporous Mesoporous Mater.* **2008**, *113*, 132. (d) Yoo, Y.; Jeong, H. K. *Chem. Commun.* **2008**, 2441. (e) Scherb, C.; Schodel, A.; Bein, T. *Angew. Chem., Int. Ed.* **2008**, *47*, 5777. (f) Kunstman, K. S.; Cyganik, P.; Goryl, M.; Zacher, D.; Puterova, Z.; Fischer, R. A.; Szymonski, M. *J. Am. Chem. Soc.* **2008**, *130*, 14446. (g) Kubo, M.; Chaikittisilp, W.; Okubo, T. *Chem. Mater.* **2008**, *20*, 2887. (h) Huang, A.; Bux, H.; Steinbach, F.; Caro, J. *Angew. Chem., Int. Ed.* **2010**, *49*, 4958.

(7) (a) Cobo, S.; Molnár, G.; Real, A. A.; Bousseksou, A. *Angew. Chem., Int. Ed.* **2006**, *45*, 5786. (b) Shekhah, O.; Wang, H.; Paradinas, M.; Ocal, C.; Schüpbach, B.; Terfort, A.; Zacher, D.; Fischer, R. A.; Wöll, C. *J. Am. Chem. Soc.* **2007**, *129*, 15118. (c) Kanaizuka, K.; Haruki, R.; Sakata, O.; Yoshimoto, M.; Akita, Y.; Kitagawa, H. *J. Am. Chem. Soc.* **2008**, *130*, 15778. (d) Shekhah, O.; Wang, H.; Kowarik, S.; Schreiber, F.; Paradinas, M.; Tolan, M.; Sternemann, C.; Evers, F.; Zacher, D.; Fischer, R. A.; Wöll, C. *Nat. Mater.* **2009**, *8*, 481. (e) Shekhah, O. *Materials* **2010**, *3*, 1302. (f) Haruki, R.; Sakata, O.; Yamada, T.; Kanaizuka, K.; Makiura, R.; Akita, Y.; Yoshimoto, M.; Kitagawa, H. *Trans. Mater. Res. Soc. Jpn.* **2008**, *33*, 629. (g) Qian, D. J.; Nakamura, C.; Ishida, T.; Wenk, S. O.; Wakayama, T.; Takeda, S.; Miyake, J. *Langmuir* **2002**, *18*, 10237.

(8) (a) Makiura, R.; Motoyama, S.; Umemura, Y.; Yamanaka, H.; Sakata, O.; Kitagawa, H. *Nat. Mater.* **2010**, *9*, 565. (b) Makiura, R.; Kitagawa, H. *Eur. J. Inorg. Chem.* **2010**, 3715.

(9) (a) Schlichte, K.; Kraskel, S. *Microporous Mesoporous Mater.* **2004**, *73*, 81. (b) Yang, L.; Kinoshita, S.; Yamada, T.; Kanda, S.; Kitagawa, H.; Tokunaga, M.; Ishimoto, T.; Ogura, T.; Nagumo, R.; Miyamoto, A.; Koyama, M. *Angew. Chem., Int. Ed.* **2010**, *49*, 5348.